

A POINT OF VIEW REGARDING TO DYNAMIC ANALYSIS OF AN AIRCRAFT STRUCTURE

Ion Fuiorea, Mihail Stoicescu

Military Technical Academy, Bucharest, Romania

Abstract

The main purpose of the work was to study the dynamic answer of the tailboom of the helicopter "ALOUETTE III" with respect to the unbalanced opposed airscrew. The study was necessary to improve the regulations of maintenance of the helicopter that operates for Romanian Airforce.

Both modal analysis and harmonic analysis were done.

In order to investigate different cases of boundary conditions and geometry solutions (for different versions of the helicopter) the authors considered first the numerical way of study. The numerical simulation of dynamic behavior of the tailboom was done by using finite element method.

Finally, for the representative cases, the authors performed some experimental determinations for numerical result validation.

During the numerical simulation the authors tested different types of elements, from compatibility point of view, and different methods for nonlinear dynamical calculations, from convergence point of view.

Essentially, the expected result of this research was the possibility of correction for some specifications of the maintenance regulations, in order to increase the flying admissible time between two technique inspections.

During the periodical control, after a certain number of flight hours, the specialists noticed frequently structural problems in the region where the tailboom was connected with the body of the helicopter (zone A in fig. 1). The problem was to study how the admissible limits of unbalanced opposed airscrew was influencing the variable stress state in the skin of the tailboom in zone A, and how the dangerous effects can be avoided.

The first study that was done refers to the dynamic analysis of tailboom taking into account the real conditions of functioning. Both modal and harmonic analysis were done.

The present paper presents only this part of study, namely the theoretical, numerical, and experimental results for the dynamical answer of the tailboom in external loading conditions, that simulate the real functioning conditions both in flight conditions and ground maintenance operations.

1. General Introduction

Romanian Airforces use different types of helicopters for logistic reasons or for other missions that do not involve them in combat procedures. One of these types is ALOUETTE III, namely its Romanian version: IAR316B.

The paper represents a part of a whole research theme that was solved in our department.



Fig. 1 The helicopter ALOUETTE III

2. Technical Considerations and Hypotheses

Because of the flexibility of the tailboom with respect to the remaining body of the helicopter (cockpit, gear compartment, etc), but especially because of simplicity, we prefer to study separately the tailboom that was considered to be fixed on a rigid platform (in three points – as it happens in real case).

This model was considered both in numerical simulation (fig. 2) and in experimental study (fig. 11) of its structure.

The static and dynamic characteristics of the materials that were used for the structure modeling were determined from the technical project of the helicopter manufacturer, namely IAR Ghimbav Brasov. No experimental determinations for these characteristics were done.

All the constitutive equations for the component materials (aluminum, titan, and magnesium alloys, steel) were considered to be linear-elastic. This hypothesis is according to the regulations for metallic aircraft structures design.

A special device was used instead of the opposed airscrew blades, that allows us to modify the unbalanced mass (see fig. 11). The device has the same inertial properties as the blades. The reason for this device using was to avoid the windy atmosphere in the laboratory during the functioning experiments.

3. Modal analysis

3.1. Numerical analysis

The numerical simulation for modal analysis of the tailboom was done by using finite element method.

3.1.1. Mathematical Model

The mathematical model of the tailboom consists in:

- geometrical model;
- model of the materials;

- finite element model;
- boundary conditions.

The *geometric model* is chosen in connection with the types of finite elements that we intend to use for structure meshing. In this acceptance, we used surfaces for skin and plate reinforcements (they will be considered plates – for modeling) and curves for strips and longerons (they will be considered beams – for modeling).

It is important to observe that the surfaces were disposed in the median surface of the skin and plates. The curves that represent a theoretic line of the beams were disposed on these surfaces. When the model of the beam will be chosen, their equations will be written with respect to this curves (uncentered and unsymmetrical), as will be discussed later.

The *model of materials* was chosen according to linear constitutive laws, as it was already mentioned.

The *finite element model* of the tailboom was done by using four element categories [1]:

- SHELL4 (SHELL3) – four noded (three noded) thin shell elements with linear interpolation functions and six DOF per node – for skin modeling, as shown in fig. 2;
- SHELL4T (SHELL3T) – four noded (three noded) thick shell elements with linear interpolation functions and six DOF per node – for thick reinforcing plates modeling, as shown in fig. 2;

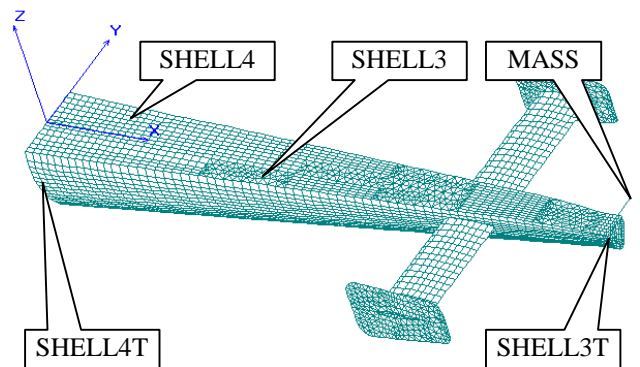


Fig. 2 Finite element model of the tailboom

- BEAM3D – three noded uncetered and unsymmetrical beam elements with

linear interpolation functions and six DOF per node – for reinforcing strips and longerons, as shown in fig. 3.

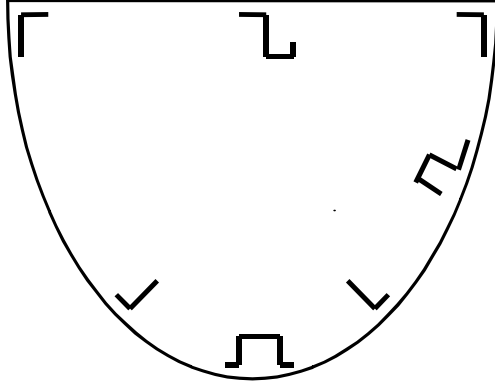


Fig. 3 Reinforcing beams

- MASS – one noded mass elements that are used to model, from inertial behavior point of view, the components that have not contribution at the structure, but their mass is considerable (for example the transmission gear box) as shown in fig. 2.

N.B. A short comment is necessary to be done:

As it was mentioned, the geometric surfaces were considered to be disposed in the median surfaces of the physical plates (skin, reinforcing plates, etc). According to this model, when these surfaces are meshed (by using SHELL elements), in FEM model, the ideal nodes are disposed in the same median surface.

On the other hand, when the reinforcing strips and longerons are modeled with finite elements (by using BEAM elements), the nodes are disposed along its median line, that in classical model lies on the centroid axis of the cross sections of the beam. The connection between the above mentioned elements in FEM model will lead to a false physical model that is shown in dotted lines in fig. 4.

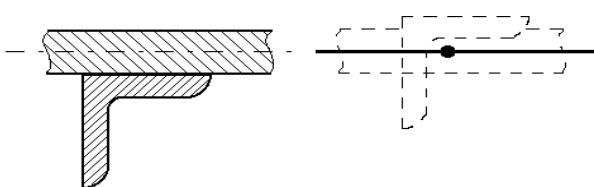


Fig. 4 BEAM-SHELL connection in a classical FEM model

This situation can be avoided if an uncentered and nsymmetric BEAM element is used. This means that the equations of this element are written with respect to a general coordinate system [2] (different of the classical one: centroidal axis).

Sequentially we can write for this general case:

$$\epsilon_{xx} = \epsilon_0 + C_{xy} z + C_{xz} y \quad (1)$$

were C_{ij} is the curvature in the plane iOj .

$$\epsilon_0 = \frac{P}{EA} - C_{xy} \bar{z} - C_{xz} \bar{y}, \quad (2)$$

$$C_{xy} = \frac{I}{E} \frac{M_z^* \cdot I_{yz}^* - M_y^* \cdot I_z^*}{I_{yz}^{*2} - I_y^* I_z^*}, \quad (3)$$

$$C_{xz} = \frac{I}{E} \frac{M_y^* \cdot I_{yz}^* - M_z^* \cdot I_y^*}{I_{yz}^{*2} - I_y^* I_z^*}. \quad (4)$$

Where

$$\begin{aligned} I_{yz}^* &= I_{yz} - \bar{I}_{yz}; & I_y^* &= I_y - \bar{I}_y; & I_z^* &= I_z - \bar{I}_z, \\ M_z^* &= M_z - \bar{M}_z; & M_y^* &= M_y - \bar{M}_y, & & \\ \bar{I}_{yz} &= \bar{y} \cdot \bar{z} \cdot A; & \bar{I}_y &= \bar{z}^2 \cdot A; & \bar{I}_z &= \bar{y}^2 \cdot A, \end{aligned} \quad (5)$$

with

$$\bar{M}_y = P \bar{z}; \quad \bar{M}_z = P \bar{y} \quad \bar{y} = \frac{S_z}{A}; \quad \bar{z} = \frac{S_y}{A}. \quad (5')$$

In conclusion, if eq (1) for reinforcing beam is written with respect to a coordinate system that passes through the median surface of the skin (for example) the connection between SHELL and BEAM elements will reflect the real case as shown in fig. 5.

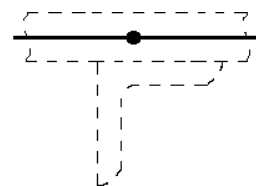


Fig. 5 BEAM-SHELL connection in uncentered and unsymmetric model

The boundary conditions model was chosen in such a way to reflect as well as possible the real conditions. As it is obvious for modal analysis only displacement boundary conditions are taken into account. According to this considerations three single pin fittings were considered symmetrical in the points where the tailboom is joined with the structure of the helicopter, as the real case.

3.1.2. Modal calculus options

The numerical calculus was done considering the following options;

- first 10 frequencies were chosen to be calculated;
- both Lanczos and Jacobi method were chosen to be used with 50 iterations;
- convergence tolerance: 1e-5;
- both lumped and consistent mass matrix were used;
- elastic connections in the joint points.

3.1.3. Numerical results

After calculations that were done for different options [3] mentioned at 3.1.2. we obtained the modal results for the first 10 modes of vibrations (frequency, dynamic deformed shape).

Because of the small torsional stiffness of the circular cross sectioned beam that is the single longeron of the horizontal tail wing, the first two modes of vibration are in close connection with its vibration. This situation is shown in fig. 6.

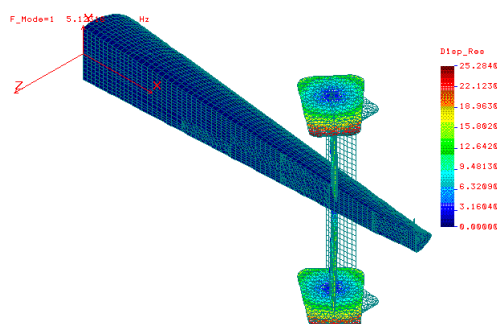


Fig. 6 Dynamic deformed shape for the first mode of vibration

In order to represent more suggestive the dynamic deformed shape of the tailboom (i.e. the displacements map) in the figures that are responsible of this illustration, the undeformed shape was designed dotted together with the undeformed elements.

As it can easy be seen, for the first mode of vibration the single part of the tailboom that participate at vibrating movement is the horizontal tail wing. The corresponding calculated frequency for this mode was

$$f_1=5.12316 \text{ Hz.}$$

A similar result, but at a 180 degree movement phase was obtained for the second mode of vibration, whose corresponding frequency was

$$f_2=5.27337 \text{ Hz.}$$

Because of their effect upon the structure, these two modes were not the subject of our study.

The modes that strongly affect the zone A of the structure (fig. 1) are the modes 3, 4 and 6.

In fig. 7 is represented the dynamic deformed shape for the third mode of vibration.

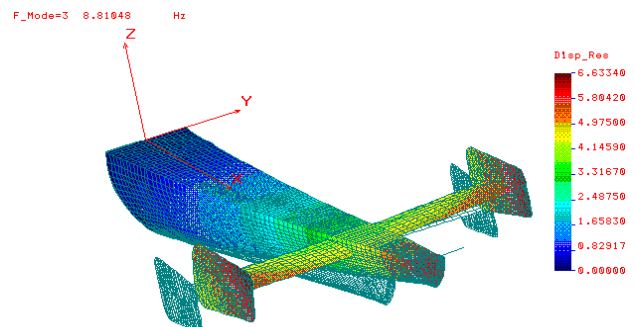


Fig. 7 Dynamic deformed shape for the third mode of vibration

The movement for this case corresponds to a bending of the tailboom as a simple beam does, around Oz axis, with a frequency

$$f_3=8.81048 \text{ Hz.}$$

It can be seen that such an alternative motion is strongly affecting the zone A of the tailboom that is suggested in fig. 1. When a harmonic analysis will be done, great values for stress will be found out.

A similar movement around Oy axis took place for the fourth mode as shown in fig. 8.

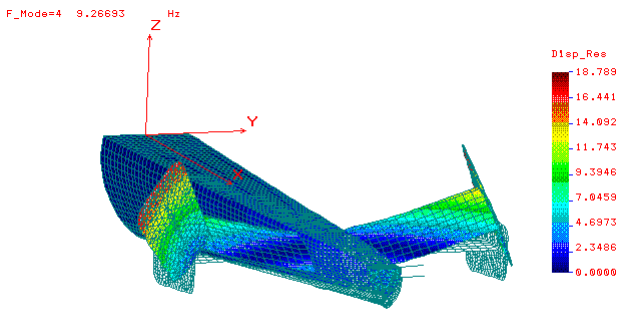


Fig. 8 Dynamic deformed shape for the fourth mode of vibration

The corresponding frequency that was calculated for this simulation was

$$f_4=9.26693 \text{ Hz.}$$

Quite a similar movement as for fourth mode of vibration can be observed for sixth mode as presented in fig. 9.

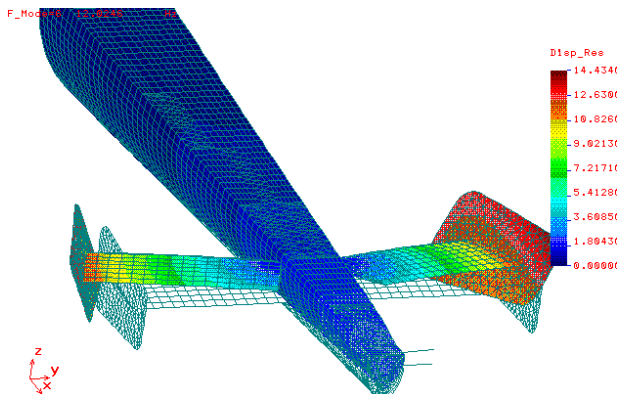


Fig. 9 Dynamic deformed shape for the sixth mode of vibration

The calculated frequency was

$$f_6=12.0246 \text{ Hz.}$$

3.2. Experimental analysis

In order to verify the value of true of the numerical simulation of the tailboom vibrations, some experiments were done for different modes of vibration.

The modes that were studied in experimental way were chosen taking into account two main reasons:

- easy applying of the exciting device;
- the simulated modes have to correspond for our interesting movements.

The method that was used in experimental analysis was the resonance method: the structure was excited in a proper point along the direction that the real vibrating movement takes place for a certain mode, and its frequency was modified until the resonance took place. Some accelerometers disposed in the points that have the maximum amplitude were used along the direction of movement.

For our study we did some experiments for the third and seventh mode of vibration (horizontal movement exciting) and for the fourth and sixth mode (vertical movement).

In fig. 10 the experimental installation together with measurement chain for the fourth and sixth mode of vibrations can be seen.

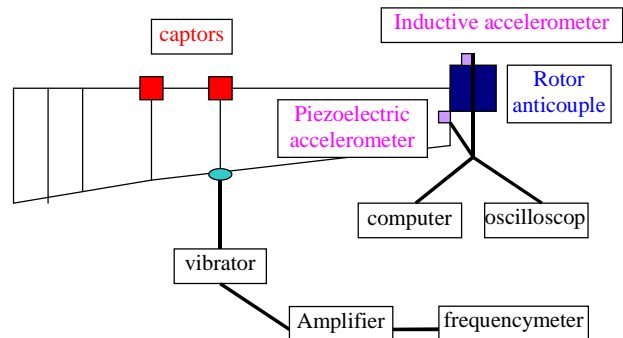


Fig. 10 Experimental scheme and measurement chain for the fourth mode of vibration

The real experimental installation is presented in fig. 11 (Laboratory of Structures of Military Aircraft Department). The structure of the tailboom can be seen together with the mounting devices that support the structure.

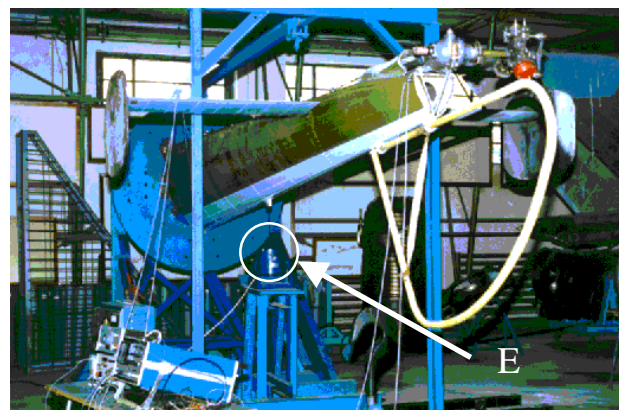


Fig. 11 Experimental installation

It is important to mention that the vibratory mass of the exciter (E in fig. 11) was enough small (150 grams). This small mass was

chosen in order to avoid the alteration of the results as a result of mass adding to the vibrating surface.

3.3. Comparative analysis

The numerical and experimental results for modal analysis are shortly presented in the following table 1.

Table 1

Mode	Frequency [Hz]		Error [%]
	Numerical	Experimental	
3	8.81048	8.42	4.64
4	9.26693	8.95	3.54
6	12.0246	12.24	1.83
7	12.4353	12.40	0.24

Some remarks are important to be done:

- the numerical results are enough precise, taking into account the purpose of our study;
- the error is decreasing with respect to the number of mode; this phenomenon can be explained by the reduced sensibility of the accelerometers for low frequencies;
- the results from numerical calculus for the other modes of vibrations can be considered acceptable.

4. Harmonic analysis

The harmonic analysis was done in order to study how the unbalanced opposed airscrew influences the dynamic answer of the structure and how the values of the unbalanced mass influence the periodic stress state in zone noted A in fig. 1.

4.1. Exciting force characteristics

The main purpose of this study was to determine the variation of displacement of a representative point of the structure with respect to the frequency of the unbalanced force, and its magnitude. The representative points of

study will be chosen as a result of modal analysis (they will be chosen in that places where their amplitudes are maximum for each particular mode).

The mathematical expression of the harmonic force was

$$\bar{F} = me\omega^2 \bar{\rho} = \begin{cases} F_x = me\omega^2 \sin\left(\omega t + \frac{\pi}{2}\right), \\ F_z = me\omega^2 \sin(\omega t) \end{cases} \quad (6)$$

where (see fig. 12)

- $\bar{\rho}$ is the rotating vector,
- me is the eccentricity,
- ω is the angular velocity of the opposed airscrew.

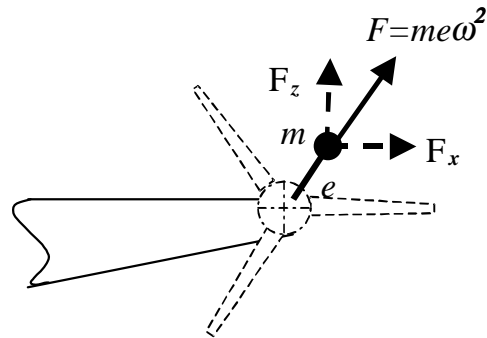


Fig. 12 Scheme of unbalanced rotating force

N.B. The values for the eccentricity were chosen from the maintenance regulations of ALOUETTE III helicopter.

In fig. 13 the diagram of exciting force is represented, with respect to the frequency.

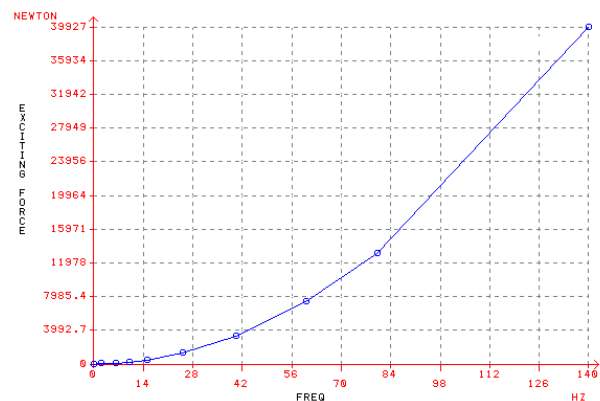


Fig. 13 Exciting force diagram

4.2. Damping characteristics

Because modal superposition method was used for harmonic analysis, the modal damping coefficients were introduced to simulate the damping phenomenon during the excited movement. In this reason the modal damping coefficients were determined in experimental way by noting the decrement of the amplitudes during free damping movement for each mode.

In fig. 14 the damped movement for the third mode of vibration is presented.

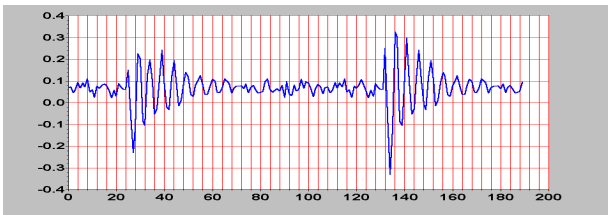


Fig. 14 Free damped vibration diagram for the third mode of vibration

If we note Δ the logarithmic decrement, we can write

$$\Delta = \ln \frac{X_1}{X_2} = \frac{2\pi\zeta}{\sqrt{1-\zeta^2}} \quad (7)$$

with

$$\zeta = \frac{C}{C_{cr}} = \sqrt{\frac{\Delta^2}{\Delta^2 + 4\pi^2}} \quad (8)$$

4.3. Numerical results

As it was previous mentioned, in present study only the displacement dynamic answer is taken into account.

The harmonic results that will be presented and analyzed later will refer to the dependence of a certain point displacement with respect to different frequencies of the exciting force that acts in the axis of opposed airscrew (as presented in fig. 12).

4.3.1. Horizontal tailboom displacements

The point situated at the extremity of tailboom was chosen for horizontal movement study.

From FEM, meshing model, the representative point is the node 12435.

In fig. 15 the function

$$u_y = u_y(f)$$

was represented for the node 12435.

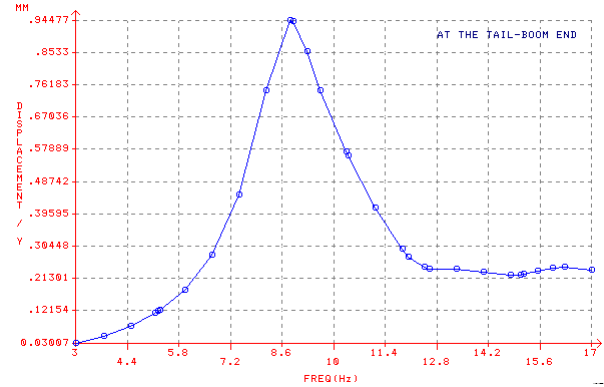


Fig. 15 Horizontal displacements of the end of tailboom in harmonic analysis

Some remarks are interesting to be do:

- maximum displacement that is obtained is corresponding to the frequency of about 9 Hz, namely the case of the third mode of vibration;
- a second pic corresponds at 13 Hz, but its amplitude is about four times smaller;
- the last one was found at 15.9 Hz, but similar from amplitude point of view;
- the next cases could not be studied because our modal analysis was done only for first 10 modes of vibration.

4.3.2. Vertical tailboom displacements

A similar analysis was done for the same node, but taking into account the vertical displacements. The results are brief presented in fig. 16.

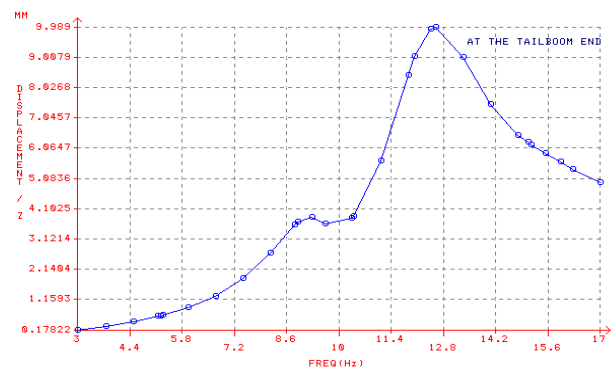


Fig. 16 Vertical displacements of the end of tailboom in harmonic analysis

In fig. 16 the function

$$u_z = u_z(f)$$

was represented for the same node 12435.

From fig. 16 we can distinguish two main local maxima:

- one around the frequency of 9 Hz, that correspond to the fourth mode of vibration;
- and the other around 12 Hz, corresponding the sixth mode, where the amplitudes are two times greater.

4.3.3. Horizontal wing displacements

Similar analysis can be done for the tailboom wings.

The representative point that was chosen corresponds to the node 8778 situated at the end of the right wing, on its top.

In fig. 17 it is represented the graphics consisting in horizontal displacements amplitude versus the exciting force frequencies

$$u_y = u_y(f).$$

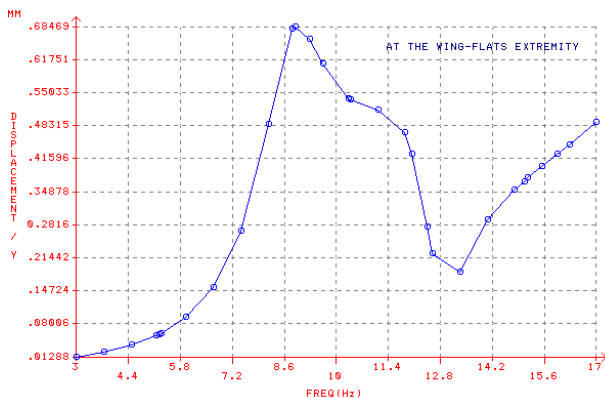


Fig. 17 Horizontal displacements of the end of tailboom wing in harmonic analysis

Maximum amplitude took place for the frequency of about 9 Hz.

4.3.4. Vertical wing displacements

Similar considerations can be done in the harmonic analysis for vertical displacements of a point situated at the end of tailboom wing, i.e. the same 8778 node. If we represent the function

$$u_z = u_z(f)$$

a certain graphic is obtained as in fig. 18.

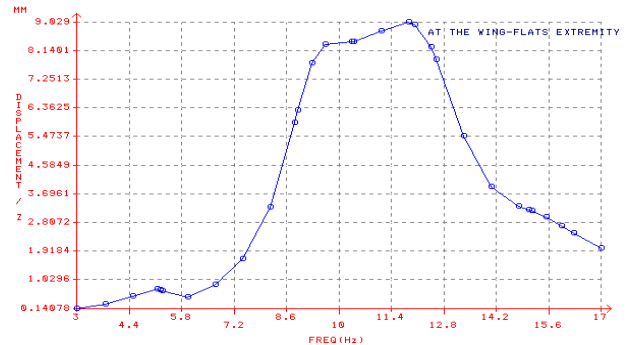


Fig. 18 Vertical displacements of the end of tailboom wing in harmonic analysis

Three main local maxims can be observed:

- the first one at about 5 Hz corresponding to the first mode of vibration;
- the second one at about 10 Hz corresponding to the fifth mode;
- and the third (the maximum) at about 12.2 Hz corresponding to the sixth mode (twelve times greater than for the first mode).

It can be concluded that in certain points it is not a rule that the amplitudes will be maximum for the frequencies that correspond to the first modes of vibration in the cases of complex structures.

References

- [1] COSMOS/M, Structural Research & Analysis Corp. *User's Guide*. California, 1999.
- [2] Rivello R. M. *Theory and analysis of flight structures*. McGraw-Hill Book Company, London, 1976.
- [3] Fuiorea I. *Finite element method for aeroelastic structures*. Military Technical Academy Ed., Bucharest, 1998.

**Military Technical Academy,
Military Aircraft Department
B-dul Regina Maria Nr. 81-83
Bucuresti, 25725, Romania
e-mail address of lead author:
ifuiorea@mta.ro**